Microbiology Research Journal International

32(5): 42-62, 2022; Article no.MRJI.90342
ISSN: 2456-7043
(Past name: British Microbiology Research Journal, Past ISSN: 2231-0886, NLM ID: 101608140)

Transcriptome Analysis of *Entamoeba histolytica* Trophozoites during *in vivo* Contact-independent Mediated Host-parasite Interaction: Putative Pathways Related to PCD

David Guillermo Pérez Ishiwara [a*], Mineko Shibayama [bω], Kumiko Nakada-Tsukui [c], Ghulam Jeelani [c], María del Consuelo Gómez-García [a], Olivia Medel Flores [a] and Tomoyoshi Nozaki [d*]

[a] Laboratorio de Biomedicina Molecular I, ENMYH, Instituto Politécnico Nacional, CP07320, Mexico.
[b] Departamento de Infectómica y Patogénesis Molecular, CINVESTAV-IPN, CP 07360, Mexico.
[c] Department of Parasitology, National Institute of Infectious Diseases, 1-23-1 Toyama, Shinjuku, Tokyo 162-8640, Japan.
[d] Department of Biomedical Chemistry, Graduate School of Medicine, The University of Tokyo, Japan.

Authors' contributions

This work was carried out in collaboration among all authors. Author DGPI did study design, drafting and the revision of intellectual content of the manuscript. Author MS did data acquisition and revision of intellectual content of the manuscript. Author KNT did data acquisition. Author GJ did data acquisition. Author MCGG did revision of intellectual content. Author OMF did data acquisition. Author TN did study design and the revision of intellectual content of the manuscript. All authors read and approved the final manuscript.

Article Information

DOI: 10.9734/MRJI/2022/v32i530390

Open Peer Review History:
This journal follows the Advanced Open Peer Review policy. Identity of the Reviewers, Editor(s) and additional Reviewers, peer review comments, different versions of the manuscript, comments of the editors, etc are available here: https://www.sdiarticle5.com/review-history/90342

Original Research Article

Received 11 June 2022
Accepted 13 August 2022
Published 18 August 2022

ABSTRACT

Aim: In the present study, we exploited DNA microarray-based transcriptome analysis and showed overall changes in gene expression *in vivo* of amoebic trophozoites that interact with animal soluble factors using an intraperitoneal dialysis bag model to elucidate putative molecular pathways and genes involved in this interaction.
Study Design: We exploited DNA microarray-based transcriptome analysis.

[ω]The author has died;
**Corresponding authors: E-mail: ishiwaramx@yahoo.com.mx, nozaki@m.u-tokyo.ac.jp;*

Results: An analysis from a network including the interactions of up-regulated genes and their neighbors revealed the presence of 11 functionally related modules. Six of the modules obtained were related to endoplasmic reticulum (ER) functions, such as degradation, stress, proteasome-ubiquitination, phosphorylation, lipid metabolism, and protein sorting. Furthermore, major transcriptional changes displayed by the parasite at the beginning of interaction were attributed to the response to the host defense. These data are consistent with the notion that the concerted expression of genes necessary for survival such as increment in protein synthesis, cytoskeleton rearrangement, vesicular traffic and genes involved in cell death including calcium imbalance and the ER signals associated with protein degradation (ERAD) is an overall landscape during the *in vivo* interaction between the amoebic trophozoites and animal soluble factors, and suggest that the ER stress is one of the main pathways leading to programmed cell death in *E. histolytica*.
Conclusion: The present findings on the global transcriptional changes displayed by the parasite at the early stages of interaction with host environments in peritoneal implantation indicate that a substantial proportion of concerted changes in gene expression in amoebic trophozoites are attributable to the parasite's response for cell death signals due to ER stress. A detailed knowledge of the underlying molecular mechanism might suggest the efficient elimination of this parasite by promoting their death pathways.

Keywords: Microarrays; E. histolytica; ER stress; programmed cell death; transcriptome; in vivo model.

1. INTRODUCTION

Amoebiasis produced by the protozoan parasite *Entamoeba histolytica* represents an important health problem especially in developing countries [1]. The mechanisms by which the parasites exert the tissue damage has been widely studied [2], and several molecular analyses have been done to understand the molecular basis of host-parasite interactions [3-5]. It is well known that the virulence of amoeba involved sequential steps, including adherence [6], contact-dependent cytolysis [7] and phagocytosis [8]. Factors involved in these processes, such as Gal/GalNac lectin subunits [9] amoebapores [4] and cysteine proteinases [5] have been described and several *in vitro* studies have demonstrated the induction of contact dependent-apoptosis in *E. histolytica* infection [10]. *In vivo,* Yan and Stanley [11], demonstrated that the use of pan-caspase inhibitor (Z-VAD-fmk) to treat mice, protect animals from amoebic liver abscess (ALA), showing a direct involvement of apoptosis in *E. histolytica* infection. On the other hand, during the destruction of host tissue, trophozoites also die. *In vitro* studies have showed the induction of Program Cell Death (PCD) after G418 aminoglycoside, hydrogen peroxide or nitric oxide exposure [12,13 and 14] and i*n vivo*, PCD has also been induced by resveratrol [15]. Villalba-Magdaleno in 2011 determined morphological features of PCD in ALA, either in parasites or in the associated host cells. Analysis of the necrotic and surrounding areas showed significant numbers of hepatocytes and inflammatory cells positive to TUNEL staining, while morphology of amoebae also correlates with rounded forms, suggesting that most of trophozoites arriving in the liver should die by PCD. TUNEL peroxidase labelling assays indicated that after 3 days post-inoculation, nuclei trophozoites were stained, indicating that PCD process was occurring [16] ALA models [17,18] represent good alternatives to study the role of PCD in the host-parasite interaction. However, as reported by Shibayama, trophozoites inoculated intraperitoneally, rapidly invade the capsule and liver parenchyma to produce tissue damage, diminishing the possibility to obtain clean and abundant samples of trophozoites and inflammatory cells to properly dissect *in vivo* PCD. TUNEL assays done in trophozoites obtained from intraperitoneal dialysis bag implantation model, demonstrated that after interaction in the peritoneum most of trophozoites within the dialysis bag were positive for TUNEL and that the concentration of nitrates and nitrites was 4 fold higher in comparison to the constant concentration in the control group, suggesting that NO could cross the membrane of the dialysis bag to induce trophozoites PCD [16]. Lin and Chadee [19] demonstrated that NO is the major cytotoxic molecule released by activated macrophages and NO-releasing molecules are effective in treating amoebiasis [20]. Other studies indicate that NO is involved in host defenses *in vivo* and that this molecule is required for the control of ALA in murine model [21]. *In vitro*, Ramos et al (2007) demonstrated

that diverse NO donors were capable of inducing apoptosis in *E. histolytica* trophozoites. The molecular pathways involved in the interphase parasite-host during interactions with the inflammatory cells have not been described. Here, using trophozoites from the intraperitoneal dialysis bag implantation model we carried out the cDNA microarray transcriptome to identify genes and cellular routes modified by the NO species or by other low mass molecules crossing the dialysis membrane, focusing our attention to those genes putative related to PCD.

2. MATERIALS AND METHODS

2.1 Parasites

Trophozoites of *E. histolytica* strain HM1: IMSS grown axenically in TYI-S-33 medium [22] were passed several times through hamster livers to increase their virulence. Virulent trophozoites were harvested at the end of the exponential growth phase (72 h) by chilling at 4°C and were used for all experiments.

2.2 Preparation of Dialysis Bags Containing Parasites

Symmetrical, cylindrical fragments of dialysis cellulose membrane (50 mm long and 7.5 mm in diameter), which were permeable for the passage of molecules up to 25 kDa (Spectrum Laboratories), were prepared under sterile conditions. After closing one end of the membrane with silk thread no. 001, 4×10^6 trophozoites were added to the bag in a total volume of 1 ml medium. The opposite side of the bag was similarly closed. These bags were maintained in sterile Petri dishes with culture medium until intraperitoneal implantation. As negative control of host-parasite interaction, the trophozoites inside the dialysis bags were incubated at 37°C into 120 ml glass bottles filled with Diamond culture medium supplemented with serum. Amoebae were recovered at 0.5, 1.5 and 3 h.

2.3 Animals

Three groups of three male golden hamsters (*Mesocricetus auratus*), aged 10–12 weeks with a mean weight of 100 g were used. The hamsters were intraperitoneally anaesthetized with sodium pentobarbital (Anestesal; Smith Kline 23) at a dose of 4.72 mg per 100 g body weight. After a mid- longitudinal incision of the abdominal wall, the dialysis bag containing 4×10^6 trophozoites in a total volume of 1 ml medium in TYI-S-33 medium [22] was introduced into the peritoneal cavity and maintained for 0.5, 1.5, and 3 h. Subsequently, the animals were sacrificed, the dialysis bags were extracted, and the trophozoites were collected. The animal management protocols were approved by the institutional committee (IACUC; number 423-08). Our institution fulfills all the technical specifications for the production, care and use of laboratory animals and is certified by national law (NOM-062- Z001999). The hamsters were sacrificed by an overdose of sodium pentobarbital at the end of the experiments and were handled according to the guidelines of the 2000 AVMA Panel of Euthanasia.

2.4 RNA Isolation and Affymetrix Microarray Hybridization

E. histolytica trophozoites obtained from intraperitoneal and control dialysis bags were collected at 0.5, 1.5, and 3 h. Three biological replicates of each condition were done. Total, RNAs were isolated from trophozoites at each experimental or control time point, by using Trizol reagent (Invitrogen, Carlsbad, CA, U.S.A.) according to the manufacturer's protocol. The RNA was quantified and the purity assessed by absorbance comparison at 260/280 nm using the NanoDrop Spectrophotometer (Thermo Scientific, Wilmington, DE, USA). The integrity of the isolated RNA was verified by using Bio-Rad's automated electrophoresis system Experion (RNA StdSens analysis kit Hercules, CA, U.S.A). All reagents and protocols are described in the Affymetrix manuals.

Briefly, total RNA (5 µg) was reverse transcribed by using T7-Oligo (dT) primer to synthetize the first strand of cDNA. After second strand synthesis, the double-stranded cDNA template was used for *in vitro* transcription, in the presence of biotinylated nucleotides to produce labeled cRNA. The cRNA was purified, quantified, fragmented, and hybridized for 16 h at 45°C to custom-generated Affymetrix platform microarray (49-7875) with probe sets consisting of 11 probe pairs representing 9,327 *E. histolytica* (Eh_Eia520620F_Eh) and 12,385 *E. invadens* open reading frames (Eh_Eia520620F_Ei). After hybridization, the arrays were washed and stained with streptavidin-phycoerythrin by using a GeneChip® Fluidics Station 450 (Affymetrix, Santa Clara, CA, USA) according to the manufacturer's instructions. After washing and staining, the

GeneChip® arrays were scanned by using the Hewlett-Packard Affymetrix Scanner 3000 (Affymetrix, Santa Clara, CA, USA), and the probe intensities were extracted by using Affymetrix®GeneChip® Command Console™ (Affymetrix, Santa Clara, CA, USA).

2.5 Analysis of Microarray Data

A minimum of two arrays was used for each condition and each time point. Raw Mas5 gene expression data were imported into the Gene Spring GX 10.0.2 program and normalized expression values for each probe set were obtained from raw probe intensities in R 2.7.0 (downloaded from the BioConductor project http:// www.bioconductor.org) by using a robust multiarray. Gene Set Enrichment Analysis (GSEA) was used for interpreting gene expression profiles, and an interactome network was built as described below.

2.6 Network Analysis

In order to explore the different biological processes and context affected by the up-regulation of a set of genes, a network analysis by using set of genes that were up-regulated (fold change >2) across the different times was performed. The network analysis was performed by using the STRING database (https://string-db.org/) and using default parameters, except text mining interactions were excluded. Thus, a network including interactions between the set up-regulated genes and their neighbors was obtained from STRING. The analysis of network was performed by using Cytoscape software (http://www.cytoscape.org/) and the MCODE plugin for module identification.

3. RESULTS

3.1 Overall Transcriptomic Profiles *in vivo* of *E. histolytica* Trophozoites using Intraperitoneal Implantation

Use of a semipermeable dialysis bag implanted in the peritoneal cavity of hamsters should allow us dissect the effects of a variety of signals given to *E.* trophozoites *in vivo* because the dialysis bag permits the exchange of small molecules, but not either large molecular weight substances > 25 kDa or interaction with mammalian cells. Using this system [16], the parasites were exposed to the peritoneal exudates in hamsters for 0.5, 1.5, and 3 h and subjected to transcriptomic analysis using DNA microarrays to obtain global expression profiles that should help us to discover genes and cellular pathways that are up- or down-regulated during interaction of the parasite with soluble factors from the host, particularly host metabolites and defense.

The transcriptomic analysis showed that 437 genes out 9327 genes were modulated by > 2 fold, among which 369 genes were upregulated and 68 genes were > 2 fold down-regulated. We detected the higher number of modulated genes in the early phase (0.5 h) of host-parasite interaction, and at later time points (1.5-3 h) the number of the genes that showed differential expression significantly decreased (Fig. 1A). An analysis from a network including the interactions of abovementioned up-regulated genes and their neighbors revealed at least 11 modules of functionally related genes (Fig. 1B). Six of these modules were associated with endoplasmic reticulum (ER) functions.

The main genes that changed in expression patterns are summarized in Tables 1 and 2.

3.2 Three Major Modules in which Upregulation of Gene Expression was Most Highly Induced

Cell signaling module represents the 34% of the up-regulated genes during contact independent host-parasite interaction, belong to this module 14% of genes involved in cytoskeletal rearrangement, such as filopodin, formin, Arp 2/3 complex activating protein rick debrin-like protein and Rho genes were found. Also genes involved in vesicle formation, transport, and trafficking, such as Dna J protein, adaptor protein, ARF GTPase activating protein, HATPase and UDP-galactose transporter genes, belongs to cell signaling, stress and protein degradation modules were highly induced. In particular, Filopodin and AP protein were >30 fold increased at 0.5 h. Other up-regulated genes grouped in protein synthesis and RNA processing modules are involved in transcription regulation, including RNA binding proteins, DNA directed RNA polymerase II large subunit, RNA recognition motif domain containing protein, transcription initiation factor SPT5, transcriptional regulator cudA, and the putative transcription factor BTF3. In particular, RNA binding protein and DNA-directed RNA polymerase II large subunit were >50 fold increased at 0.5 h (Fig. 2, Table 1).

Table 1. List of most highly up-regulated genes at one or more-time point

Probe set ID	Accession numbers	Common Name	Basal Expression (log2)	0.5 h		Fold Change 1.5 h		3 h	p-value
EHI_053170_at	XM_652031	RNA-binding protein, putative	6.75	+	57.94	+	33.74	+ 30.96	8.1E-05
EHI_121760_at	XM_646689	DNA-directed RNA polymerase II large subunit, putative	3.77	+	56.21	+	38.12	+ 36.57	5.6E-04
EHI_059870_s_at	XM_647804	hypothetical protein	5.31	+	36.91	+	13.74	+ 25.77	4.7E-04
EHI_167130_at	XM_649685	filopodin, putative	5.08	+	36.35	+	14.18	+ 30.43	1.5E-04
EHI_131980_at	XM_647514	DnaJ domain containing protein	2.32	+	35.72	+	3.91	+ 25.41	5.8E-04
EHI_023600_at	XM_644199	adaptor protein (AP) family protein	6.49	+	30.30	+	8.33	+ 33.59	1.6E-04
EHI_111550_at	XM_643969	hypothetical protein	5.82	+	30.17	+	7.91	+ 35.13	1.1E-04
EHI_056700_at	XM_643998	hypothetical protein	3.56	+	30.15	+	3.91	+ 22.46	1.9E-04
EHI_098580_at	XM_650875	hypothetical protein	3.61	+	27.96	+	8.97	+ 17.00	1.3E-03
EHI_167710_at	XM_650468	apoptosis-linked gene 2 interacting protein X homolog family member (alx-1)*	3.19	+	26.48	+	12.30	+ 24.00	4.4E-04
105.m00129_s_at	XM_647676	hypothetical protein	3.78	+	25.62	+	6.13	+ 20.60	4.8E-04
EHI_197440_at	XM_646593	suppressor protein SRP40*	6.77	+	25.60	+	26.58	+ 26.33	1.3E-04
EHI_188820_at	XM_651565	formin 2,3 and collagen domain-containing protein*	3.90	+	25.43	+	4.11	+ 19.72	1.3E-03
EHI_000260_at	XM_647653	RNA recognition motif domain containing protein	2.98	+	25.43	+	5.78	+ 20.15	3.3E-03
EHI_067890_at	XM_651689	Ras guanine nucleotide exchange factor, putative	4.82	+	24.97	+	15.25	+ 22.60	4.6E-04
72.m00162_s_at	XM_648701	hypothetical protein	3.72	+	24.15	+	5.24	+ 22.78	8.9E-04
EHI_190990_s_at	XM_001914546	diaphanous protein, putative	2.67	+	24.03	+	4.86	+ 16.54	3.1E-03

Probe set ID	Accession numbers	Common Name	Basal Expression (log2)	0.5 h		Fold Change 1.5 h		3 h	p-value
935.m00010_s_at	XM_642761	hypothetical protein	2.58	+	23.60	+	15.17	+	8.43	7.0E-04
EHI_189170_at	XM_644224	calcium-binding protein*	4.63	+	23.46	+	4.54	+	11.63	5.6E-04
EHI_186120_s_at	XM_001914572	ARF GTPase activating protein*	2.45	+	22.46	+	4.98	+	12.77	4.7E-04
EHI_187280_at	XM_651366	transcription initiation factor SPT5, putative	5.43	+	22.36	+	15.04	+	14.68	4.6E-04
EHI_114770_at	XM_645230	putative mucin binding protein*	6.12	+	21.97	+	14.45	+	15.28	5.5E-04
EHI_014910_s_at	XM_001914428	hypothetical protein	3.79	+	21.41	+	5.47	+	2.54	8.3E-04
EHI_197520_at	XM_646601	glutenin, low molecular weight subunit precursor*	5.20	+	19.03	+	12.89	+	15.88	8.3E-05
EHI_162570_at	XM_646653	ornithine cyclodeaminase, putative	2.77	+	18.90	+	10.09	+	13.97	2.7E-03
EHI_068440_at	XM_649065	hypothetical protein	5.16	+	18.50	+	4.20	+	18.60	7.5E-04
195.m00089_s_at	XM_645764	hypothetical protein	8.24	+	18.00	+	3.17	+	18.93	8.6E-05
EHI_016130_at	XM_651324	Arp2/3 complex-activating protein rickA*	6.43	+	17.79	+	3.65	+	21.33	3.7E-04
EHI_103410_at	XM_647331	W D domain containing protein	7.21	+	17.59	+	6.97	+	17.93	9.3E-05
EHI_134850_at	XM_647045	Fe-hydrogenase*	3.72	+	17.49	+	11.62	+	29.22	8.7E-05
EHI_125900_at	XM_651394	hypothetical protein	4.23	+	17.39	+	10.53	+	11.15	5.1E-04
EHI_084710_at	XM_650002	hypothetical protein	3.13	+	17.37	+	8.30	+	3.32	1.9E-03
EHI_007000_at	XM_649353	Arp2/3 complex-activating protein rickA*	5.24	+	16.61	+	3.59	+	14.11	4.9E-04
EHI_069480_at	XM_643857	HEAT repeat domain containing protein	5.99	+	16.30	+	11.52	+	12.69	8.3E-05
EHI_039850_at	XM_646872	Rho guanine nucleotide exchange factor, putative	5.81	+	16.12	+	10.88	+	6.90	1.3E-04
EHI_093920_at	XM_652186	calcium-binding protein*	2.84	+	15.99	+	21.89	+	53.21	2.1E-03
EHI_194180_at	XM_649627	hypothetical protein	5.73	+	15.71	+	6.04	+	19.68	8.9E-04
EHI_025470_at	XM_647866	hypothetical protein	5.40	+	15.34	+	14.27	+	15.16	8.1E-05
328.m00063_s_at	XM_644142	hypothetical protein	4.75	+	15.14	+	14.88	+	16.76	1.1E-03

Probe set ID	Accession numbers	Common Name	Basal Expression (log2)	0.5 h		Fold Change 1.5 h		3 h	p-value
EHI_004350_at	XM_647164	hypothetical protein	5.25	+	14.87	+	5.43	+	9.12	2.4E-04
EHI_110770_at	XM_649183	hypothetical protein	4.99	+	14.68	+	2.65	+	2.81	1.5E-02
EHI_178970_at	XM_651197	cdc-2 related kinase 3*	5.86	+	14.44	+	2.11	+	13.59	2.2E-04
EHI_095050_at	XM_648381	Arf GTPase activating protein	5.07	+	13.95	+	3.70	+	12.37	1.1E-04
EHI_015980_at	XM_650992	hypothetical protein	3.00	+	13.80	+	6.81	+	3.31	1.5E-03
EHI_100080_at	XM_646625	acid sphingomyelinase-like phosphodiesterase, putative	4.79	+	13.65	+	14.28	+	10.75	1.4E-04
EHI_078740_at	XM_646344	Rho guanine nucleotide exchange factor, putative	5.17	+	13.46	+	5.25	+	8.34	6.2E-04
EHI_131890_at	XM_647521	hypothetical protein	6.96	+	13.42	+	4.61	+	11.17	5.1E-04
EHI_069180_at	XM_650187	Rho GTPase activating protein, putative	4.79	+	13.27	+	5.27	+	16.06	9.5E-04
3.m00619_s_at	XM_652158	hypothetical protein	8.64	+	13.08	+	13.94	+	12.96	8.5E-04
EHI_170170_at	XM_650881	rap/ran GTPase-activating protein*	5.95	+	13.04	+	7.13	+	10.09	1.6E-04
EHI_135460_at	XM_644409	Tumor susceptibility gene 101 protein*	3.59	+	13.03	+	7.61	+	6.59	1.6E-04
EHI_045090_s_at	XM_001913357	pyruvate, phosphate dikinase*	6.91	+	12.90	+	12.63	+	13.10	1.9E-03
EHI_099330_at	XM_646662	Acidic proline-rich protein PRP33 precursor*	2.89	+	11.96	+	4.72	+	10.67	1.7E-03
EHI_100400_s_at	XM_646609	DNA-repair protein, putative	3.49	+	11.78	+	9.36	+	8.06	8.1E-04
EHI_066720_at	XM_646043	hypothetical protein	4.38	+	11.49	+	10.26	+	13.54	2.0E-04
EHI_052730_at	XM_646543	transcriptional regulator cudA*	2.32	+	11.47	+	6.84	+	10.18	9.7E-04
EHI_068650_at	XM_645417	hypothetical protein	8.14	+	11.43	+	3.69	+	10.99	9.6E-05
EHI_029600_at	XM_644990	hypothetical protein	5.86	+	11.42	+	3.37	+	8.59	5.8E-04
EHI_019060_s_at	XM_001913963	DNA mismatch repair protein mutS, putative	3.39	+	11.37	+	3.27	+	7.57	2.7E-04
EHI_056090_at	XM_647505	UDP-galactose	4.05	+	11.36	+	9.23	+	9.71	2.8E-04

Probe set ID	Accession numbers	Common Name	Basal Expression (log2)	Fold Change 0.5 h		1.5 h		3 h	p-value
		transporter*							
EHI_041960_at	XM_651434	haloacid dehalogenase-like hydrolase	6.11	+	11.13	+	8.07	+	9.58	6.9E-04
50.m00196_s_at	XM_649450	hypothetical protein	6.33	+	10.92	+	3.76	+	2.06	3.0E-04
EHI_030420_at	XM_644725	tyrosine kinase, putative	4.45	+	10.83	+	4.58	+	6.46	4.0E-04
EHI_173500_at	XM_644049	hypothetical protein	6.87	+	10.81	+	6.32	+	6.09	4.4E-04
EHI_198870_at	XM_649900	transcription factor BTF3, putative	7.08	+	10.79	+	6.88	+	6.33	1.2E-03
EHI_131930_at	XM_647518	Rho GTPase activating protein, putative	5.28	+	10.52	+	10.22	+	10.16	1.6E-04
EHI_165220_at	XM_647140	adhesin 112*	4.62	+	10.44	+	7.40	+	8.94	1.0E-03
EHI_079950_at	XM_647784	Wiskott-Aldrich syndrome protein*	6.13	+	10.32	+	2.75	+	19.52	2.3E-04
EHI_117860_at	XM_650978	Dedicator of cytokinesis domain containing protein*	4.68	+	10.24	+	7.53	+	6.43	5.3E-04
311.m00024_s_at	XM_644281	hypothetical protein	5.72	+	10.21	+	11.13	+	10.14	4.6E-04
EHI_187080_at	XM_651386	hypothetical protein	5.85	+	10.19	+	5.46	+	6.52	2.2E-04
194.m00119_s_at	XM_645798	hypothetical protein	4.34	+	10.02	+	7.98	+	8.85	3.0E-04
EHI_023330_at	XM_650547	HATPase_c domain-containing protein*	7.17	+	5.82	+	20.62	+	2.21	2.1E-04
873.m00008_at	XM_642788	hypothetical protein	3.01	+	5.59	+	17.43	+	3.33	1.1E-02
490.m00041_s_at	XM_643193	hypothetical protein	7.13	+	5.39	+	16.62	+	13.85	9.9E-04
EHI_014810_at	XM_643227	hypothetical protein	3.49	+	8.43	+	14.93	+	8.42	5.5E-04
EHI_126660_at	XM_001914527	hypothetical protein	4.19	+	5.10	+	13.69	+	13.66	2.4E-04
EHI_049570_at	XM_650791	RhoGAP domain containing protein	5.51	+	9.05	+	12.53	+	10.61	2.2E-04
EHI_159710_at	XM_645157	alanine aminotransferase, putative	5.03	+	7.85	+	10.66	+	8.30	2.0E-03
EHI_135120_at	XM_646563	DENN domain-containing protein 2D*	5.24	+	9.75	+	10.52	+	12.39	9.7E-05
EHI_152280_at	XM_651890	serine palmitoyltransferase, putative	8.01	+	9.21	+	10.25	+	11.14	1.3E-04

Probe set ID	Accession numbers	Common Name	Basal Expression (log2)	Fold Change 0.5 h		Fold Change 1.5 h		Fold Change 3 h		p-value
EHI_110620_at	XM_649167	zinc finger domain containing protein	6.72	+	8.44	+	10.24	+	11.39	1.8E-04
EHI_054800_at	XM_646985	Drebrin-like protein*	7.53	+	9.19	+	10.04	+	9.04	3.0E-04
131.m00151_s_at	XM_647018	hypothetical protein	5.27	+	7.44	+	5.10	+	12.69	1.2E-03
EHI_109880_at	XM_647114	hypothetical protein	4.21	+	3.59	+	8.04	+	11.54	4.1E-03

The probe set IDs, accession numbers, common names, basal expressions, fold changes, and p values of most highly down-regulated genes are shown Only genes that shown >2-fold changes any time point are shown. The genes are sorted in a descending order of the fold change at 30 min.
**Annoted as hypothetical protein in genome database. Common name assigned based on blast results*

Table 2. List of most highly down-regulated genes at one or more-time point

Probe set ID	Accession numbers	Common Name	Basal pression (log2)	0.5 h		Old Change				p-value
						1.5 h		3 h		
EHI_014320_at	XM_649990	adenosine deaminase, putative	10.09	–	11.53	–	4.18	–	2.26	2.4E-04
EHI_192580_at	XM_648805	TATA-binding protein-associated phosphoprotein*	7.81	–	11.31	–	3.17	–	2.97	1.1E-03
28.m00338_s_at	XM_650365	Hypothetical protein	7.71	–	10.99	–	9.93	–	2.95	6.1E-04
EHI_183280_at	XM_650378	DnaJ family protein	7.49	–	9.36	–	8.57	–	2.40	2.4E-03
EHI_061760_at	XM_643432	protein folding regulator*	6.48	–	8.95	–	7.19	–	1.62	1.2E-02
585.m00015_at	XM_642978	Hypothetical protein	11.49	–	8.35	–	6.72	–	7.03	3.1E-03
EHI_038300_at	XM_648611	Hypothetical protein	9.35	–	8.19	+	1.25	–	1.12	1.0E-03
EHI_096610_at	XM_651845	zinc finger protein*	7.71	–	7.52	–	1.40	–	1.58	5.1E-04
EHI_168310_at	XM_645838	myb-like DNA-binding domain containing protein	6.06	–	7.50	–	1.56	–	3.66	5.5E-03
EHI_006850_at	XM_649369	histidine kinase*	6.79	–	7.11	–	10.71	–	9.46	2.0E-04
EHI_019140_at	XM_648030	FkbM family methyltransferase*	5.84	–	7.05	–	8.60	–	3.41	5.3E-03
EHI_141050_at	XM_001913802	TATA-binding protein-associated phosphoprotein*	6.94	–	6.24	–	2.22	–	2.45	1.9E-02
EHI_178050_at	XM_646404	ATP-binding cassette protein, putative	9.41	–	6.04	+	1.70	–	4.64	2.1E-04
EHI_003950_at	XM_643818	LigB subunit of aromatic ring-opening dioxygenase*	9.32	–	5.87	–	3.61	–	5.05	1.9E-04
183.m00115_s_at	XM_645998	Hypothetical protein	7.86	–	5.68	–	2.17	–	2.76	4.9E-02
EHI_011980_at	XM_651119	splicing factor, arginine/serine-rich*	6.86	–	5.60	–	1.65	–	6.60	1.2E-02
EHI_010130_at	XM_651999	small GTP-binding protein*	9.78	–	5.60	–	4.49	–	2.90	7.2E-04
EHI_180160_x_at	XM_648730	peptidyl-prolyl cis-trans isomerase, FKBP-type , putative	5.34	–	5.43	–	1.66	–	1.87	4.4E-02
EHI_125980_at	XM_645324	TATA-binding protein-associated phosphoprotein*	8.67	–	5.38	–	2.30	–	6.22	2.3E-04
EHI_081240_at	XM_651719	cell wall surface anchor family protein*	5.37	–	5.35	–	1.72	–	1.60	7.4E-03
EHI_072240_s_at	XM_001914512	glucose-6-phosphate isomerase, putative	7.57	–	5.27	–	3.83	–	1.81	4.7E-04

Probe set ID	Accession numbers	Common Name	Basal pression (log2)	0.5 h		Old Change 1.5 h		3 h		p-value
EHI_102270_s_at	XM_648070	heat shock protein 90, putative	10.45	–	5.24	–	4.57	–	1.32	6.7E-04
EHI_105320_at	XM_648851	histidine kinase*	6.02	–	5.22	–	4.08	–	5.20	6.0E-03
EHI_049800_at	XM_652090	TATA-binding protein-associated phosphoprotein*	8.41	–	5.15	–	2.08	–	2.76	5.6E-04
EHI_137050_at	XM_647500	S-adenosylmethionine-diacylglycerol 3-amino-3-carboxypropyl transferase*	9.91		5.08	–	2.35	–	2.27	2.0E-03
EHI_004820_s_at	XM_645616	Regulator of nonsense transcripts 1 like protein*	11.41	–	4.32	–	16.10	–	2.45	3.3E-04
EHI_120360_at	XM_001913983	grainin, putative	12.32	–	3.12	–	11.96	–	3.43	5.4E-05
EHI_050290_at	XM_643501	SGS domain protein	7.64	–	4.59	–	6.67	–	2.10	2.6E-04
829.m00009_x_at	XM_642814	Hypothetical protein	5.52	–	3.62	–	5.28	–	1.48	5.0E-02
EHI_005040_at	XM_647744	adenosine deaminase, putative	7.59	–	2.38	–	5.21	–	2.49	3.2E-04
EHI_055680_at	XM_646949	heat shock protein, Hsp20 family, putative	6.33	–	1.59	–	5.14	+	1.08	1.8E-03
EHI_051440_at	XM_646199	peptide synthetase*	7.59	–	1.73	–	4.71	–	7.17	1.7E-02
EHI_011380_at	XM_643745	transporter, auxin efflux carrier (AEC) family	7.80	–	1.09	–	1.55	–	6.93	2.4E-04
EHI_110700_at	XM_649176	sucrose transporter, putative	5.88	–	2.56	–	2.47	–	6.80	4.9E-02
EHI_136430_at	XM_650171	ribonuclease R*	7.33	–	3.93	–	1.75	–	6.40	1.6E-03
434.m00036_x_at	XM_643458	Hypothetical protein	5.39	+	1.38	+	1.17	–	6.27	2.2E-02
EHI_067230_x_at	XM_647567	ACT domain-containing protein*	7.36	–	3.35	–	1.73	–	5.67	8.3E-05
EHI_093910_at	XM_652187	histidine triad (hit) protein*	8.85	–	1.39	–	3.60	–	5.23	3.0E-02
EHI_070010_at	XM_643695	RAD52 motif-containing protein 1-like isoform 1*	4.68	–	3.30	–	2.16	–	5.14	2.8E-03

The probe set IDs, accession numbers, common names, basal expressions, fold changes, and p values of most highly down-regulated genes are shown Only genes that shown >2-fold changes any time point are shown. The genes are sorted in a descending order of the fold change at 30 min.
**Annoted as hypothetical protein in genome database. Common name assigned based on blast results.*

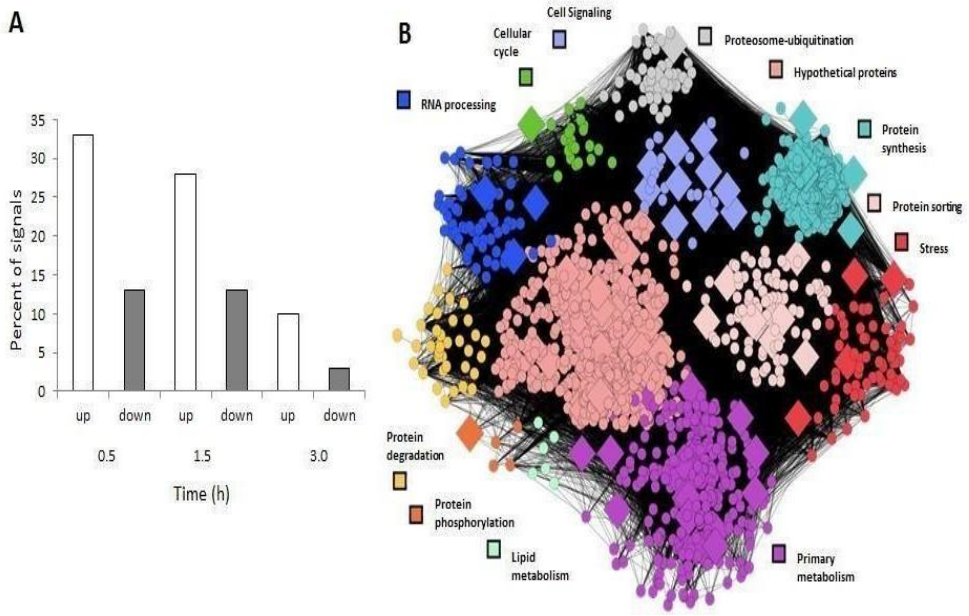

Fig. 1. Signals modulated during host-parasite interactions A. Expression percentage of genes at each time of host-parasite interaction. Each bar indicates the percentage of genes that are upregulated or downregulated from microarray analysis. B. Graphic representation of the network analysis

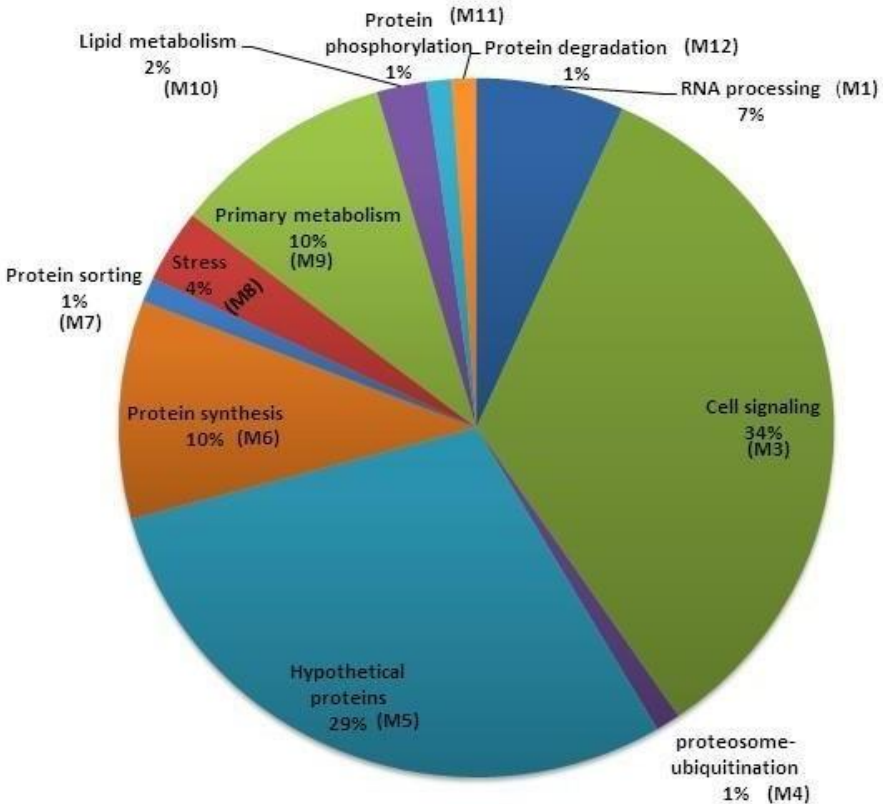

Fig. 2. Representative percentage of the up-regulated genes grouped by modules (M) according to functions inferred from network analysis

3.3 Gene Expression Changes Involved in Programmed Cell Death

Two genes involved in PCD in other organisms, such as apoptosis-linked gene 2 and alx-1 (interacting protein X homolog family member) were also detected. Interestingly, a calcium binding protein showed a continuous hike in the expression from 16 to 53-fold during 3 h. It should be noted that 29% of the up-regulated genes were annotated as hypothetical proteins (Figs. 1, 3).

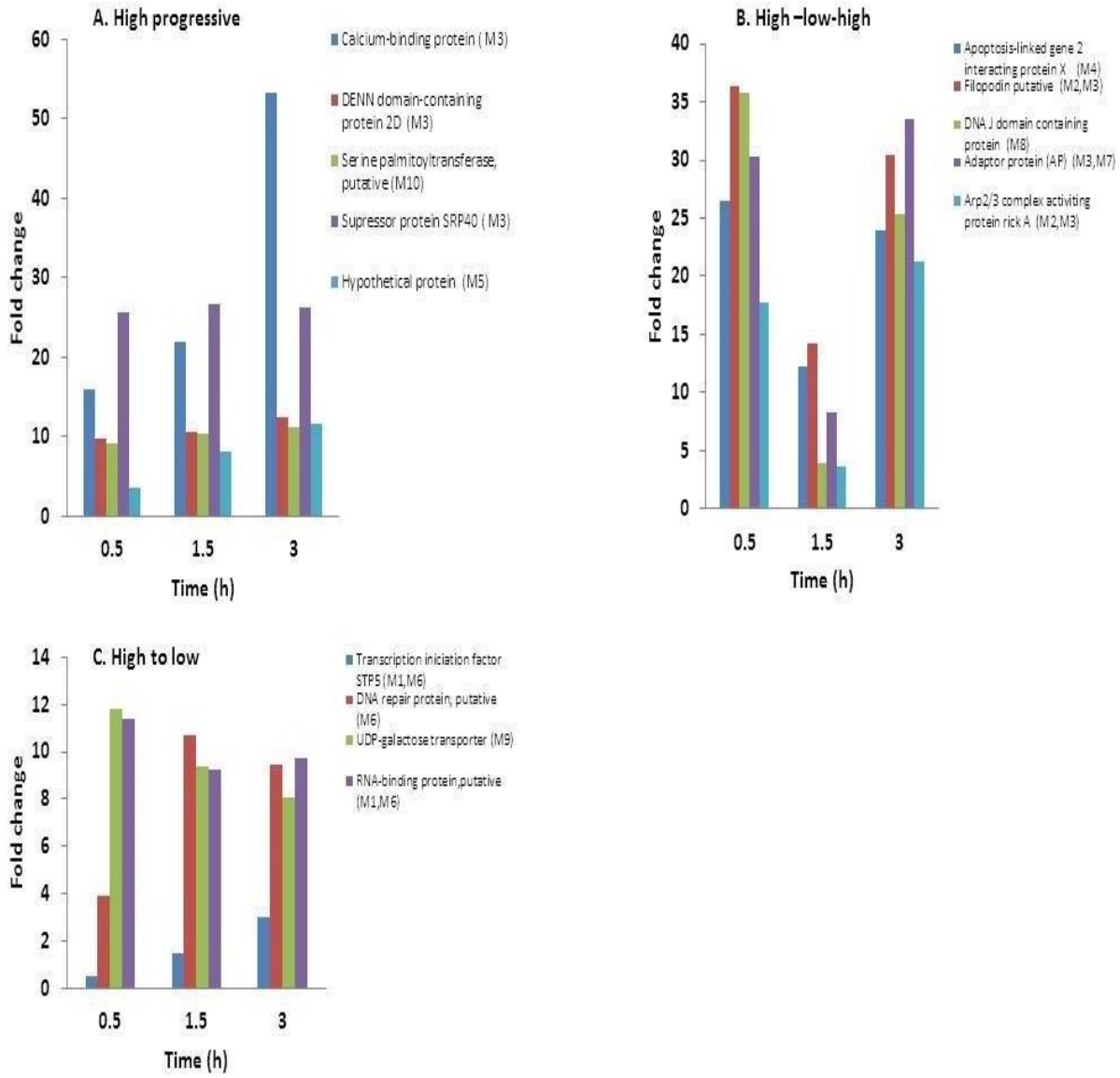

Fig. 3. Expression pattern profiles of representative up-regulated genes from some modules

*Transcript expression changes at 0.5, 1.5 and 3 h of contact independent host-parasite interaction **A**. High progressive: EHI_093920, Calcium-binding protein (p=2.1E-03); EHI_135120, DENN domain- containing protein 2D (p=9.7E-05); EHI_152280, Serine palmitoyltransferase, putative (p=1.3E-04); EHI_197440, Suppressor protein SRP40 (p=1.3E-04); EHI_109880, Hypothetical protein (p=4.1E-03). **B**. High-low-high: EHI_167710, Apoptosis-linked gene 2 interacting protein X homolog family member (alx- 1) (p=4.4E-04); EHI_167130, Filopodin, putative (p=1.5E-04); EHI_131980, DnaJ domain containing protein (p=5.8E-04); EHI_023600, Adaptor protein (AP) family protein (p=1.6E-04); EHI_016130, Arp2/3 complexactivating protein rickA (p=4.9E-04) and **C**. High to low: EHI_187280, Transcription initiation factor SPT5, putative (p=4.6E-04); EHI_100400, DNA-repair protein, putative (p=8.1E-04); EHI_056090, UDP-galactose transporter (p= 2.8E-04); EHI_053170, RNA binding protein, putative (p=8.1E-05)*

3.4 Kinetics of Transcriptional Changes of Upregulated Genes

Results presented in Fig. 3 show different profiles of expression modulation of representative genes from some modules. Calcium binding protein, DENN- domain containing protein 2D from module involved in cell signaling; serine palmitoyltransferase and suppressor protein SRP40 from lipid metabolism and cell signal modules, respectively, displayed high progressive up- modulation increasing continuously its expression during the 3 h of experimentation. Other genes related to cell death signals, cytoskeletal rearrangement, stress and protein sorting, such as Apoptosis-linked gene 2 interacting protein, Filopodin, Dna J domain containing protein, Adaptor protein (AP) and Arp 2/3 complex activating protein rick A, displayed an interesting modulation pattern in which its expression was high at the beginning of host parasite interaction, decreasing in average 3 fold at 1.5 h. Followed by gene expression up-regulation at 3 h. Finally, there was an expression pattern in which a group of genes (Transcription initiation factor SPT5, DNA repair protein, UDP-galactose transporter and RNA binding protein) from proteosome-ubiquitination, cell signaling, protein synthesis and primary metabolism modules diminished continuously during the 3 h of experimentation (Fig. 3).

On the other hand, we observed that 16 % of the downregulated (>2 fold) genes are involved in transcription, such as TATA-binding protein-associated phosphoprotein, myb-like, splicing factor, regulator of nonsense transcript 1 like protein, ribonuclease R. Among them, TATA-binding protein associated phosphoprotein showed a largest extent of repression (11.5-fold increase at 0.5 h). Additionally, 20 % of the downregulated genes are involved in metabolism module, such as adenosine deaminase, histidine kinase, Fkb family methyltransferase and glucose 6-phosphate isomerase. Adenosine deaminase showed a largest extent of repression (11.3-fold decrease at 0.5 h). Thirty-three percent of the downregulated genes, such as heat shock proteins 90 and 20 and a RAD52 motif containing protein 1-like isoform, protein folding regulation and grainin, are involved in stress response to DNA damage; cell signaling, proteosome ubiquitination and protein degradation modules. Eighteen percent of down regulated genes were hypothetical proteins (Fig. 4).

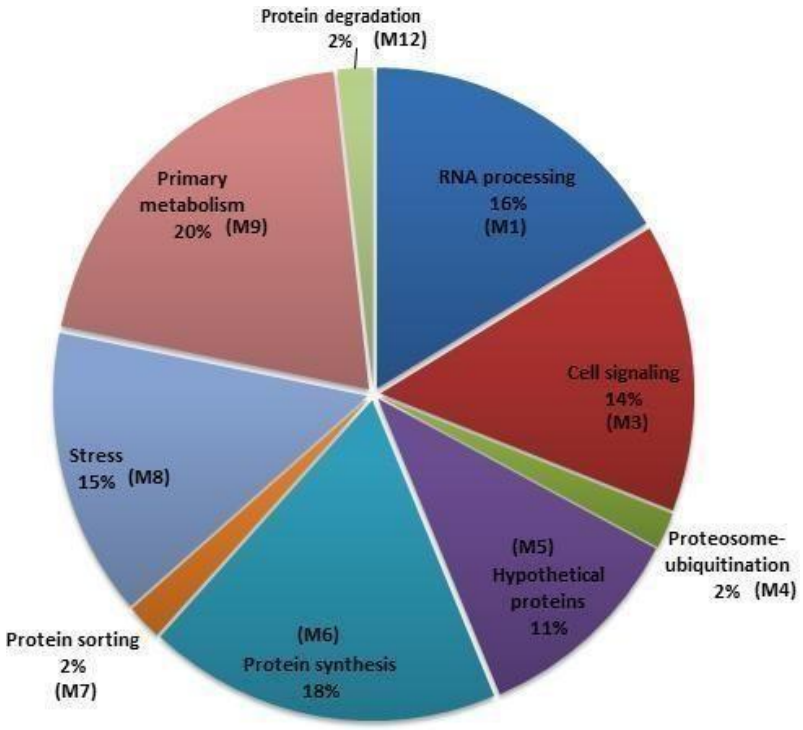

Fig. 4. Representative percentage of the down-regulated genes grouped by modules (M). according to functions inferred from network analysis

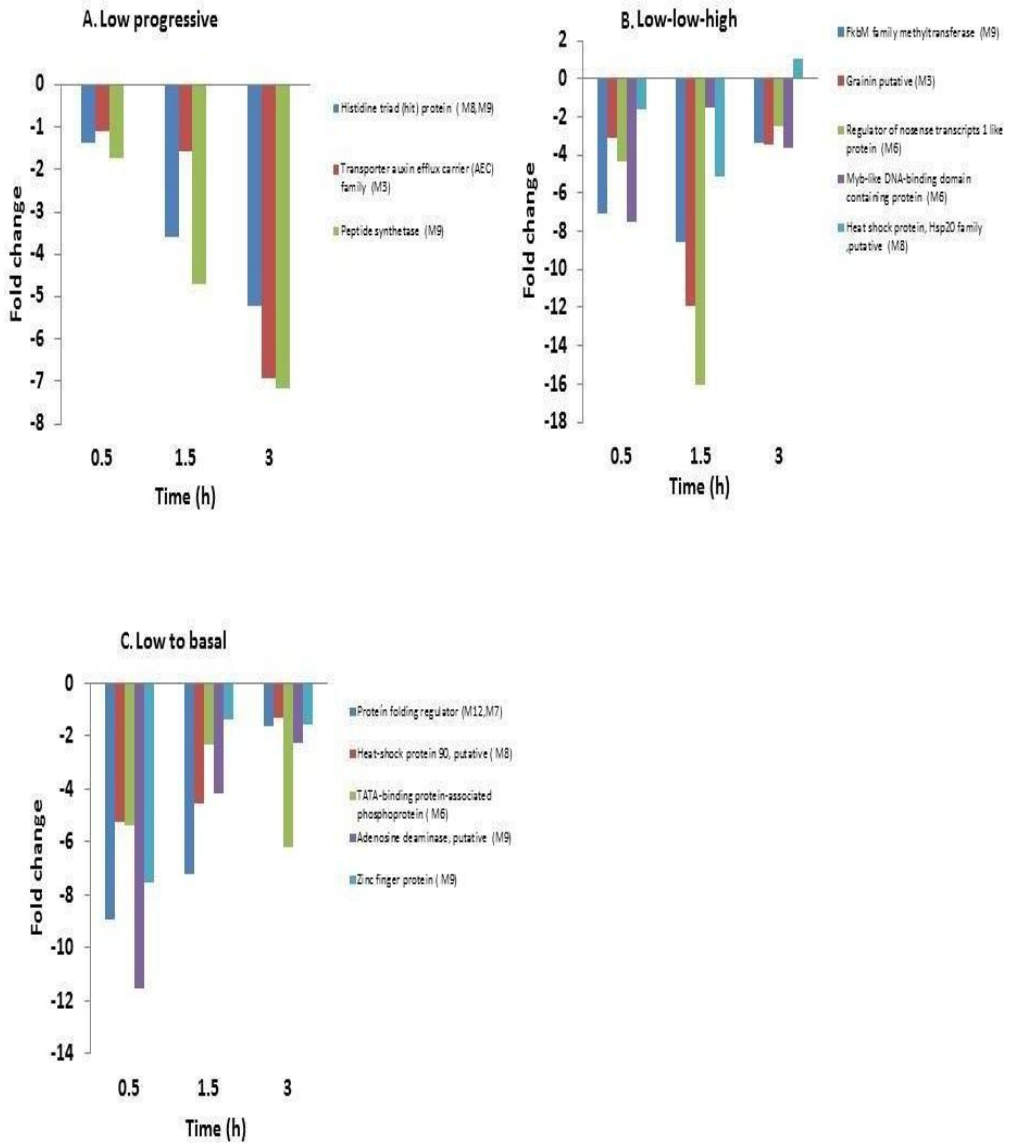

Fig. 5. Expression pattern profiles of representative down-regulated genes from some modules
Transcript expression changes at 0.5, 1.5 and 3 h of contact independent host-parasite interaction. ***A****. Low progressive: EHI_ 093910, Histidine triad (hit) protein (p=3.OE-02); EHI_ 011380, Transporter, auxin efflux Carrier (AEC) Family (p=2.4E-04); EHI_051440, Peptide synthetase (p=1.7E-02)* ***B.*** *Low-low-to basal: EHI_019140, FkbM family methyltransferase (p= 5.3E-03); EHI_ 120360, Grainin, putative (p= 5.4E-05); EHI_ 004820, Regulator of nonsense transcripts 1 like protein (p=3.3E-04); EHI_ 168310, Myb- like DNA binding domain containing protein(p=5.5E-03); EHI_ 055680, Heat shock protein, Hsp20 family putative (p=1.8E-03) and* ***C****. Low to basal: EHI_ 061760, Protein folding regulator (p= 1.2E-02); EHI_ 102270, Heat shock protein 90, putative (p=6.7E-04); EHI_ 125980, TATA-binding protein-associated phosphoprotein (p= 2.3E-04); EHI_ 014320, Adenosine deaminase, putative (p=2.4E-04) ; EHI_ 096610, Zinc finger protein(p= 5.1E-04)*

3.5 Kinetics of Transcriptional Changes of Down-regulated Genes

The representative patterns of most highly downregulated genes are shown in Table 1 and Fig. 5. Among 39 genes, 26 genes showed a transient decrease in the corresponding transcript at 0.5 h, but the expression was recovered after 1.5 h. In contrast, 4 genes, represented by peptide synthetase (EHI_051440_at), transporter auxin efflux carrier (AEC) family (EHI_011380_at), histidine triad (hit) protein (EHI_093910_at) and hypothetical protein (434.m00036_x_at) showed continuous decrease in expression. While 9 genes showed a transient decrease until 0.5 h, but the expression was recovered after 3 h. Fig. 5 show different profiles of expression modulation of

representative genes from some modules. Protein folding regulator, Heat shock protein 90, TATA-binding protein-associated phosphor-protein, Adenosine deaminase and Zinger finger protein from modules of protein degradation, protein sorting, stress, protein synthesis and primary metabolism, displayed low to high modulation expression pattern, from an important low expression going back to basal expression pattern at 3 h. Other genes related to primary metabolism, calcium regulator, transcription and stress, displayed a modulation pattern in which its low expression at the beginning was enhanced 1.5 h later to recovered it after 3 h. Finally, there was an expression pattern in which a group of genes (histidine triad (hit) protein, transporter auxin efflux carrier (AEC) family, peptide synthetase from modules of cell signaling, stress and primary metabolism displayed a continuously and progressive turned off during the 3 h of experimentation (Fig. 5).

Interestingly, some genes related to ER functions, such as a calcium binding protein (calcium homeostasis) (EHI_093920_at), DENN domain containing protein 2D (vesicular traffic) (EHI_135120_at), and putative serine palmitoyltransferase (lipid biosynthesis) (EH_152280_at), maintained similar expression levels through all interaction times.

4. DISCUSSION

Intraperitoneal implantation of dialysis bag containing trophozoites represents an alternative and useful model to properly dissect molecular effectors and cellular pathways in response to host-parasite interactions [16], due conventional intraperitoneal model of ALA production [17] has the inconvenient to recover very few samples of trophozoites and inflammatory cells to analyze the host parasite interaction at molecular level. Moreover, the factors operating in this peritoneal milieu are multiple and difficult to relate directly to specific events.

Major transcriptomic response observed during the exposure of amebic trophozoites to intraperitoneal environment.

In the present study, we used the intraperitoneal implantation model [16] to identify genes that could be involved in contact-independent and low molecular substance-mediated host-parasite interactions, with a particular aim at the discovery of the key genes that could play role in PCD of the amoeba. Transcriptomic analyses revealed a complex modulation of parasite gene expression during the interaction with the host intraperitoneal exudate. The highest extent of modulation of gene expression was seen at the early interaction (0.5 h) compared to later time points (1.5-3 h), suggesting that the majority of the responses was to the adaptation to environmental changes, such as low molecular substances such as ions, metabolites, and radicals. Besides the various patterns of modulation were also saw higher expression changes (e.g., continuous or transient up or down regulation), suggesting that the adaptation to the new environment requires the concerted complex action of variety of genes and pathways. The interactome analysis of intraperitoneal implanted trophozoites revealed 11 main functionally related modules of differentially expressed genes. The primary metabolism and protein synthesis modules were the largest groups of interacting members, representing the 53% of the interactions within the network, without considering the hypothetical proteins module. Interestingly, we also observed modules related to protein degradation, stress, proteasome-ubiquitination, protein phosphorylation, lipid metabolism and protein sorting that could be associated with endoplasmic reticulum (ER) functions between other cellular activities.

Causal connection between ER stress and PCD during the exposure of amoebic trophozoites to the intraperitoneal environment.

The ER is indispensable in all eukaryotes including *E. histolytica* [10]. The ER is involved in many cellular functions, including translation, protein folding and secretion, lipid biosynthesis, and importantly calcium homeostasis [23]. Many factors are known to perturb ER functions and induce the ER stress including: excessive protein synthesis and misfolding above the capacity of protein chaperones, calcium release from stores, and disturbance of the redox balance and oxidative stress [24]. Here, we suggested that transcriptomic changes observed in the amoebic trophozoites within intraperitoneal implantation bags could be related to ER stress, in particular, the modules of protein synthesis and transcription, as shown by the interactome analysis. Moreover, we also identified some transcriptomic changes that are often observed in the intracellular calcium imbalance such as cytoskeleton rearrangement and vesicular traffic, reinforcing the notion that the trophozoites were exposed to ER stress in peritoneal implantation.

This observation agrees well with our previous reports in which the triggers that induce PCD *in vitro* concomitantly caused calcium release from the ER, increasing intracellular calcium concentrations, and increasing the expression and activity of some PCD-related proteins including calpain [12,25,14,26]. In another study, we modelled a hypothetical 3D structure of the E. histolytica calpain-like protein, based on the conserved domains previously identified in the primary sequence of the protein [26]. Using Western blot (WB) analysis and confocal microscopy, we demonstrated that calpain-like protein expression increased during PCD induction, localizing the protein to the cytoplasm and close to the nucleus. Knockdown of the calpain gene using a specific RNA interference (siRNA) sequence caused a 65% decrease in PCD. These results support the hypothesis that the calpain-like protein plays an important role in the PCD execution phase of E. histolytica. Furthermore, a hypothetical interactome of the calpain-like protein suggests that other proteins, including some with calcium-binding domains, also participate in the PCD pathway of this parasite [27].

The expression of grainin, which is a calcium binding protein located in the cytoplasmic granules [28] that was previously reported to increase during PCD [25], was downregulated. However, our previous studies have suggested that grainins 1 and 2 could play important roles at the beginning of G418-induced PCD *in vitro*, as suggested by the increase in the expression of grainin genes at 0.5 h and rapidly decrease in expression at 1.5 h [25]. The transcriptomic analysis in the present study showed a progressive overexpression of a calcium-binding protein (EHH_093920) in a course of peritoneal implantation (16- and 53-fold at 0.5 and 3 h, respectively). *In vivo,* other calcium-binding protein such as fortilin in human is also known to be involved in calcium capture [29]. Thus, it is likely that the profuse imbalance of calcium during host parasite interaction requires, in addition to grainins, the participation of a more efficient calcium capture mechanism(s) not identified yet. Other studies have suggested that changes in the intracellular calcium concentrations controls cytoskeleton rearrangement [30], associated with modulation of gene expression of their regulators [31-34]. These reports seem to agree to our observation that the genes encoding for filopodin, formin, Arp 2/3 complex activating protein rick, debrin-like protein, and Rho genes, which are involved in cytoskeletal rearrangement and vesicular traffic, were positively modulated during the intraperitoneal implantation.

4.1 Decrease in HSP Expression and Stress Response

We have also shown that the expression of Hsp90 and Hsp20 decreased, suggesting that trophozoites were under stress responses. Similarly, the downregulation of Hsp90 in insects has been associated with a stress response to the parasites [35]. Conversely, in adult worms of the parasitic nematode *Nippostrongylus brasiliensis,* the diminished expression of Hsp90 was observed in response to host immunity during infection [36]. Evidence that Hsp90 plays a role in the host-parasite interface has also been suggested in *Eimeria tenella*, in which the expression of Hsp90 was enhanced during the invasion of host cells, while the inhibition of Hsp90 activity led to a significant reduction in the invasion capacity of the parasite [37]. Moreover, the simultaneous reduction of expression of Hsc70 and Hsp70 in human cancer cell lines inhibited Hsp90 function and cell proliferation and induced apoptosis [38].

4.2 Link between NO and PCD

Production of NO species by the host plays an important role in the mammalian immune system by killing or inhibiting the growth of many pathogens, including parasites, virus and bacteria [39]. In the intraperitoneal dialysis bag implantation model, NO produced and released by macrophages and neutrophils were evaluated. In serum, peritoneal cavity and the supernatant contained within the bag, the concentration of nitrates and nitrites were 9 to 16, 6 to 7, and 4 to 5 folds higher, respectively, in the group of stimulated hamsters in comparison to the constant concentration in the control group. The higher NO concentration suggest that NO could cross the membrane of the dialysis bag to induce trophozoites PCD [16]. Lin and Chadee [19] demonstrated that NO is the major cytotoxic molecule released by activated macrophages and NO-releasing molecules are effective in treating amoebiasis [20]. Other studies indicate that NO is involved in host defenses *in vivo* and also NO is required for the control of ALA in murine model [21]. *In vitro*, Ramos et al [13] demonstrated that diverse NO donors were capable of inducing apoptosis in *E. histolytica* trophozoites. Santi-Rocca *et al,* also examined amoebic gene expression during the *in vitro*

incubation of parasites with NO. The data revealed changes in expression, predominating upregulation of the genes associated with membrane traffic, extreme stress responses, cysteine metabolism, and anaerobic energy production [40]. *In vivo* experiments, some currently in progress, may employ specific nitric oxide synthase (NOS) inhibitors, such as N^6-nitro- 1argimethyl ester (L-NAME), amino guanidine and dexamethasone, or possibly NOS Knockout mice will allow us to determine if inhibition of NO production cancel the transcriptional response that depends upon NO in the peritoneal exudate.

4.3 Link between ER Stress and Membrane Traffic

ER stress induces the increment of vesicles formation and protein transport [41]. The microarray analysis in the present study showed that during intraperitoneal implantation, the genes involved in vesicular trafficking, Rab and Arf small GTPases, Arf GTPase activating protein, RhoGAP domain containing protein, and DENN domain-containing protein 2D [42,43] retained consistent upregulated expression levels throughout the course of experiments (3 h). Also, the adaptor protein (AP) complex family, which is involved in protein sorting in the endomembrane system of eukaryotic cells [44], is also upregulated (30 fold at 0.5 h). This evidence is consistent with the hypothesis that one of the main responses within trophozoites after host interaction is a concerted expression phenomenon induced by ER stress [31].

The unfolded protein response and upregulation of ER-associated protein degradation components during peritoneal implantation.

The cells adapt to ER stress by activating an integrated signal transduction pathway called the unfolded protein response (UPR). The UPR represents a survival response by the cells to restore ER homeostasis. The ability of cells to respond against perturbations in ER stress is critical for cell survival, but chronic or unresolved ER stress can lead to apoptosis [45]. One important consequence of UPR is the upregulation of ER-associated protein degradation components (ERAD) [46]. In the present study, we detected the modulation of several signals involved in UPR and ERAD: i) the overexpression of DnaJ, a molecule responsible for the modulation of protein assembly/disassembly and translocation in eukaryotes [47] ii) the adaptor protein (AP) complex family involved in protein sorting in the endomembrane system [42] iii) the downregulation of hypothetical proteins folding regulator; and iv) HATPase responsible for acidification of intracellular compartments in eukaryotes [48]. The modulation of HATPase gene expression agrees well with the acidification of endosomes detected in *E. histolytica* during PCD *in vitro* [12,49]. In higher eukaryotes, ER-stress-mediated apoptosis involves caspase-12 activation by calpain [50]. It was previously reported in *E. histolytica* that the overexpression and increased activity of calpain-like proteases during the induction of PCD *in vitro and in vivo* were triggered by the calcium imbalance [26,51,15,13,14]. In addition, we also detected a signal involved in PCD, such as the apoptosis-linked gene product, ALG-2, a member of the family of intracellular calcium binding proteins, which has been demonstrated as directly linked to apoptosis in higher eukaryotes [52,53].

5. CONCLUSION

Programmed Cell Death (PCD) represents a very important mechanism in the early stages of parasite-host interaction. During this process, we propose that cellular and molecular events triggered by the parasite are determinant for the success of the infection and the viability of the parasite. On the one hand, to induce host cell death, in particular of immune cells, without causing inflammation, and on the other hand to protect against host-induced PCD against the parasite. The present findings on the global transcriptional changes displayed by the parasite in the early stages of interaction with diffusible host factors, simulated in peritoneal implantation, indicated that a substantial proportion of the concerted changes in gene expression of amoebic trophozoites are attributable to the parasite's response to cell death signals due to ER stress. A detailed understanding of the underlying molecular mechanism could suggest pathways that promote effective trophozoite clearance that aid in the control and eradication of amebiasis.

ACKNOWLEDGEMENTS

This work was supported by grants from the Instituto Politécnico Nacional to DGPI.

COMPETING INTERESTS

Authors have declared that no competing interests exist.

REFERENCES

1. World Health Organization (WHO). 'A consultation with experts on amebiasis', Epidem. Boll PAHO. 1997;18:13-4.
2. Marie C, Petri WA Jr. Regulation of virulence of Entamoeba histolytica. Annu Rev Microbiol. 2014;68:493-520.
3. Ravdin JI, Stanley P, Murphy CF, Petri WA Jr. Characterization of cell surface carbohydrate receptors for Entamoeba histolytica adherence lectin. Infect Immun. 1989;57(7):2179-86.
4. Leippe M, Ebel S, Schoenberger OL, Horstmann RD, Müller-Eberhard HJ. Pore-forming peptide of pathogenic Entamoeba histolytica. Proc Natl Acad Sci U S A. 1991;88(17):7659-63.
5. Que X, Reed SL. Cysteine proteinases and the pathogenesis of amebiasis. Clin Microbiol Rev. 2000;13(2):196-206.
6. Petri WA Jr., Smith RD, Schlesinger PH, Murphy CF, Ravdin JI. Isolation of the galactosebinding lectin that mediates the in vitro adherence of Entamoeba histolytica. J Clin Invest. 1987;80(5):1238-44.
7. Huston CD, Houpt ER, Mann BJ, Hahn CS, Petri WA Jr. Caspase 3-dependent killing of host cells by the parasite Entameba histolytica. Cell Microbiol. 2000;2(6):617-25.
8. Orozco E, Guarneros G, Martínez-Palomo A, Sánchez T. Entamoeba histolytica. Phagocytosis as a virulence factor. J Exp Med. 1983;158(5):1511-21.
9. Petri WA Jr., Haque R, Mann BJ. The bittersweet interface of parasite and host: lectin carbohydrate interactions during human invasion by the parasite Entamoeba histolytica. Annu Rev Microbiol. 2002;56:39-64.
10. Teixeira JE, Huston CD. Evidence of a continuous endoplasmic reticulum in the protozoan parasite Entamoeba histolytica. Eukaryot Cell. 2008;7(7):1222-6.
11. Yan L, Stanley SL Jr. Blockade of caspases inhibits amebic liver abscess formation in a mouse model of disease. Infect Immun. 2001;69(12):7911-4.
12. Villalba JD, Gómez C, Medel O, Sánchez V, Carrero JC, Shibayama M et al. Programmed cell death in Entamoeba histolytica induced by the aminoglycoside G418. Microbiology (Reading). 2007; 153(11):3852-63.
13. Ramos E, Olivos-García A, Nequiz M, Saavedra E, Tello E, Saralegui A, et al. Entamoeba histolytica: apoptosis induced in vitro by nitric oxide species. Exp Parasitol. 2007;116(3):257-65.
14. Nandi N, Sen A, Banerjee R, Kumar S, Kumar V, Ghosh AN, et al. Hydrogen peroxide induces apoptosis-like death in Entamoeba histolytica trophozoites. Microbiology (Reading). 2010;156(7):1926-41.
15. Pais-Morales J, Betanzos A, García-Rivera G, Chávez-Munguía B, Shibayama M, Orozco E. Resveratrol induces apoptosis-like death and prevents in vitro and in vivo virulence of Entamoeba histolytica. Plos One. 2016;5:2-23.
16. Villalba-Magdaleno JD, Pérez-Ishiwara G, Serrano-Luna J, Tsutsumi V, Shibayama M. In vivo programmed cell death of Entamoeba histolytica trophozoites in a hamster model of amoebic liver abscess. Microbiology (Reading). 2011;157(5):1489-99.
17. Shibayama M, Campos-Rodríguez R, Ramírez-Rosales A, Flores-Romo L, Espinosa-Cantellano M, Martínez-Palomo A et al. Entamoeba histolytica: liver invasion and abscess production by intraperitoneal inoculation of trophozoites in hamsters, Mesocricetus auratus. Exp Parasitol. 1998;88(1):20-7.
18. Shibayama M, Rivera-Aguilar V, Barbosa-Cabrera E, Rojas-Hernández S, Jarillo-Luna A, Tsutsumi V et al. Innate immunity prevents tissue invasion by Entamoeba histolytica. Can J Microbiol. 2008;54(12):1032-42.
19. Lin JY, Chadee K. Macrophage cytotoxicity against Entamoeba histolytica trophozoites is mediated by nitric oxide from L-arginine. J Immunol. 1992;148(12):3999-4005..
20. Sannella A, Gradoni L, Persichini T, Ongini E, Venturini G, Colasanti M. Intracellular release of nitric oxide by NCX 972, a NO-releasing metronidazole, enhances in vitro killing of Entamoeba histolytica. Antimicrob Agents Chemother. 2003;47(7):2303-6.
21. Seydel KB, Smith SJ, Stanley SL Jr. Innate immunity to amebic liver abscess is dependent on gamma interferon and nitric oxide in a murine model of disease. Infect Immun. 2000;68(1):400-2.

22. Diamond LS, Harlow DR, Cunnick CC. A new medium for the axenic cultivation of Entamoeba histolytica and other Entamoeba. Trans R Soc Trop Med Hyg. 1978;72(4):431-2.
23. Schröder M. Endoplasmic reticulum stress responses. Cell Mol Life Sci. 2008;65(6):862-94.
24. Ron D, Walter P. Signal integration in the endoplasmic reticulum unfolded protein response. Nat Rev Mol Cell Biol. 2007;8(7):519-29.
25. Monroy VS, Flores MO, Villalba-Magdaleno J, D, García CG, Ishiwara DG. 'Entamoeba histolytica: differential gene expression during programmed cell death and identification of early pro- and anti-apoptotic signals'. Exp. Pasitol. 2010;126:497-505.
26. Monroy VS, Flores OM, García CG, Maya YC, Fernández TD, Pérez IDG" Calpain-like: A Ca(2) dependent cystein protease in Entamoeba histolytica". Exp. Pasitol. 2015;159:245-51.
27. Dominguez F-, Rodriguez M.A., Sánchez Monroy V., Gómez García C., Medel O., Pérez Ishiwara D.G. "A calpain-like protein is involved in the execution phase of Programmed Cell Death in Entamoeba histolytica". Front Cell Infect. Microbiol. 2018;8:1-11.
28. Nickel R, Jacobs T, Urban B, Scholze H, Bruhn H, Leippe M. MTwo novel calcium-binding proteins from cytoplasmic granules of the protozoan parasite Entamoeba histolytica. FEBS Lett. 2000;486(2):112-6.
29. Graidist P, Yazawa M, Tonganunt M, Nakatomi A, Lin CC, Chang JY et al. Fortilin binds Ca^{+2} and blocks Ca^{+2} dependent apoptosis in vivo. Biochem J. 2007;408(2):181-91.
30. Nalefski EA, Falke JJ. 'The C2 domain calcium-binding motif: structural and functional diversity. Protein', Sci. Protein Sci. 1996;5(12):2375-90.
31. Bosch DE, Siderovski DPG. Protein Signals in the parasite Entamoeba histolytica. Exp Mol Med. 2013;45:e15.
32. Mujumber S, Lohia A. Entamoeba histolytica encodes unique formins, a subset of which regulates DNA content and cell division. Infect Immun. 2008;76:368-2378.
33. Schönichen A, Alexander M, Gasteier JE, Cuesta FE, Fackler OT, Geyer M. Biochemical characterization of the diaphonous autoregulatory interaction in the formin homology protein FHOD1. J Biol Chem. 2006;281(8):5084-93.
34. Goode BL, Rodal AA, Barnes G, Drubin DG. Activation of the Arp2/3 complex by the actin filament binding protein Abp1p. J Cell Biol. 2001;153(3):627-34.
35. Zhu JY, Wu GX, Ye GY, Hu C. Heat shock protein genes (hsp20, hsp75 and hsp90) from Pieris rapae: molecular cloning and transcription in response to parasitization by Pteromalus puparum. Insect Sci. 2013;20(2):183-93.
36. Arizono N, Yamada M, Tegoshi T, Takaoka Y, Ohta M, Sakaeda T. HSp12.6 expression is inducible by host immunity in adult worms of the parasitic nematode Nippostrongylus brasiliensis. PLOS ONE. 2011;3:1814-10.1371.
37. Péroval M, Péry P, Labbé M. The heat shock protein 90 of Eimeria tenella is essential for invasion of host cell and schizont growth. Int J Parasitol. 2006;36(10-11):1205-15.
38. Powers MV, Clarke PA, Workman P. Dual targeting of HSC70 and HSP72 inhibits HSP90 function and induces tumor-specific apoptosis. Cancer Cell. 2008;14(3):250-62.
39. Chakravortty D, Hensel M. Inducible nitric oxide synthase and control of intracellular bacterial pathogens. Microbes Infect. 2003;5(7):621-7..
40. Santi-Rocca J, Weber C, Pineda E, Hon CC, Saavedra E, Olivos-García A, et al. Endoplasmic reticulum stress-sensing mechanism in Entamoeba histolytica upon treatment with nitric oxide. PLOS ONE. 2012;7:e31777.
41. Schindler AJ, Schekman R. In vitro reconstitution of ER-stress induced ATF6 transport in COPII vesicles. Proc Natl Acad Sci U S A. 2009;106(42):17775-80.
42. Marat AL, Dokainish H, McPherson PS. DENN domain proteins: regulators of Rab GTPases. J Biol Chem. 2011;286(16):13791-800.
43. Imai A, Ishida M, Fukuda M, Nashida T, Shimomura H "MADD/ DENN/Rab3GEP functions as a guanine nucleotide exchange factor for Rab27 during granule exocytosis of rat parotid acinar cells". Arch Biochem. 2013;536:31-7.
44. Mattera R, Park SY, De Pace R, Guardia CM, Bonifacino JS. AP-4 mediates export of ATG9A from the trans-Golgi network to promote autophagosome formation. Proc

Natl Acad Sci U S A. 2017;114(50):E10697-706.
45. Szegezdi E, Logue SE, Gorman AM, Samali A. Mediators of endoplasmic reticulum stress induced apoptosis [EMBO rep]. EMBO Rep. 2006;7(9):880-5.
46. Schröder M. The unfolded protein response. Mol Biotechnol. 2006;34(2):279-90.
47. Walsh P, Bursac D, Law YC, Cry D, Lighgow T. The j-protein family: modulating protein assembly, disassembly and translocation [EMBO rep]. 2004;6:567-71.
48. Forgac M. Structure and function of vacuolar class of ATP-driven proton pumps. Physiol Rev. 1989;69(3):765-96.
49. Medel Flores O, Gómez García C, Sánchez Monroy V, Villalba Magadaleno JD, Nader García E, Pérez Ishiwara DG. Entamoeba histolytica P-glycoprotein (EhPgp) inhibition, induce trophozoite acidification and enhance programmed cell death. Exp Parasitol. 2013;135(3): 532-40.
50. Nakagawa T, Yuan J. Cross-talk between two cysteine protease families. Activation of caspase-12 by calpain in apoptosis. J Cell Biol. 2000;150(4):887-94.
51. Ghosh AS, Dutta S, Raha S. Hydrogen peroxide-induced apoptosis-like cell death in Entamoeba histolytica. Parasitol Int. 2010;59(2):166-72.
52. Lo KW, Zhang Q, Li M, Zhang M. Apoptosis-linked gene product ALG-2 is a new member of the calpain small subunit subfamily of Ca2+- binding proteins. Biochemistry. 1999;38(23):7498-508.
53. Gannavaram S, Debrabant A. Programmed cell death in Leishamania: biochemical evidence and role in parasite infectivity. Front Cell Infect Microbiol. 2012;2:95.

Peer-review history:
The peer review history for this paper can be accessed here:
https://www.sdiarticle5.com/review-history/90342